

Elastic and nonelastic deformation of greensand

ZAKIR HOSSAIN and IDA LYKKE FABRICIUS, *Technical University of Denmark*
 HELLE FOGED CHRISTENSEN, *Danish Geotechnical Institute*

Analysis of greensand reservoirs all over the world has challenged geologists, engineers, and petrophysicists. One challenge is to identify from core data the degree to which deformation of the reservoir rock affects hydrocarbon production. In the central part of the North Sea, massive allocthonous Paleocene greensands form reservoirs for oil. We study the deformation of one oil-zone sample from one of these reservoirs by sonic measurements, uniaxial compression testing, and image analysis of backscatter electron micrographs before and after testing.

Greensands are a mixture of stiff clastic grains, macropores, and soft microporous glauconite grains. The studied Paleocene greensand contains 22% iron-bearing illitic glauconite, 60% quartz, feldspar, and the iron-bearing 7Å clay berthierine. Macropores reside between these grains (Figure 1a), whereas the glauconite grains enclose micropores (Figure 1b). The deformation properties of these mineralogically heterogeneous sands reflect the properties of their constituents.

Deformation properties of a rock can be determined from geotechnical compression testing and from sonic measurements. The main differences between the two types of tests are the frequency of deformation and the strain amplitude. When an acoustic wave propagates through a porous medium, the frequency is relatively high and the strain amplitude is low, so the deformation of the porous medium is elastic. In a static test, the frequency is low and the strain amplitude is large. So, in a porous medium, a nonelastic deformation as well as an elastic deformation can arise. Nonelastic deformation comprises closing of microcracks formed during retrieval of the core and grains sliding into a denser packing or, for greensands, a permanent deformation of glauconite grains.

Elastic deformation may be described by Young's modulus and Poisson's ratio. When during geomechanical compression, a static uniaxial stress (σ) is applied, the axial deformation (ϵ_z) is determined from the loading curve, and where strain gauges are applied, the radial strain $\epsilon_x = \epsilon_y$ may also be obtained. For a linearly elastic material, Hooke's law states:

$$d\epsilon_z = \frac{d\sigma}{E_{static}} \quad (1)$$

where the coefficient E_{static} is the static Young's modulus. The static Poisson's ratio, ν_{static} , describes the radial to axial strain and is defined as:

$$\nu_{static} = -\frac{d\epsilon_x}{d\epsilon_z} \quad (2)$$

The elastic deformation caused by propagation of sonic waves may be calculated from P-wave velocity (v_p), S-wave

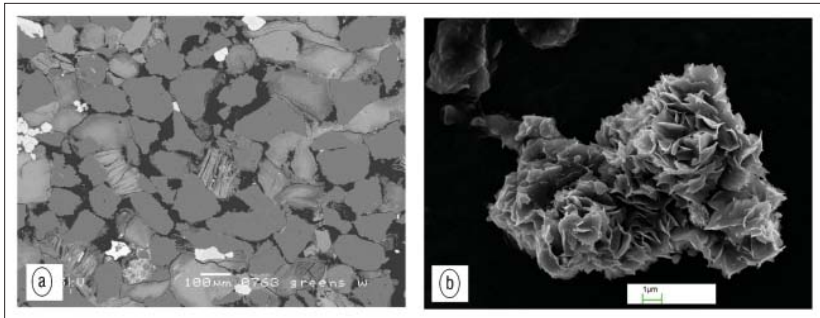


Figure 1. (a) BSE image of the North Sea greensand and (b) glauconite grain from Arnager greensand. Scale bar for greensand is 100 μm, and the image represents macroporosity, quartz, and glauconite grains. Scale bar for glauconite grain is 1 μm. Micropores reside within glauconite grain.

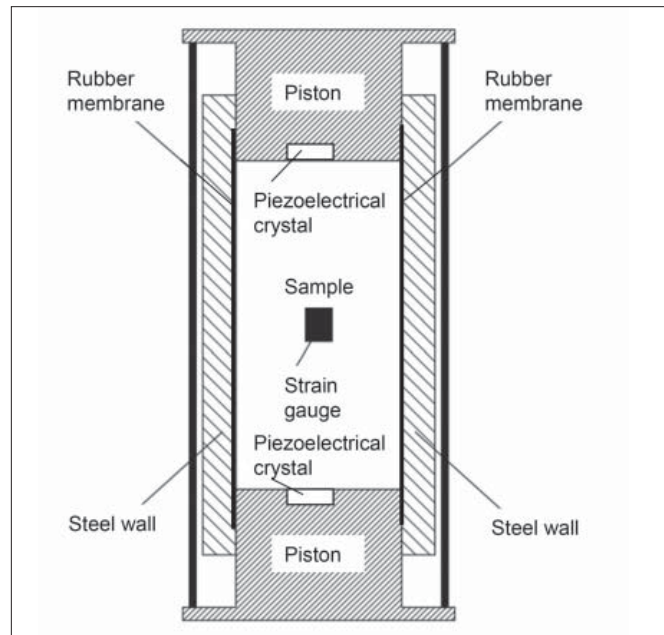


Figure 2. Triaxial cell. Strain gauges measure axial and radial strain. Confining pressure is controlled by hydraulic oil. Piezoelectric crystals are built into the pistons for continuous measuring of P-wave and S-wave velocity during compression tests. (Modified after Olsen et al.)

velocity (v_s), and density (ρ), of the rock, as expressed in the dynamic Young's modulus, $E_{dynamic}$:

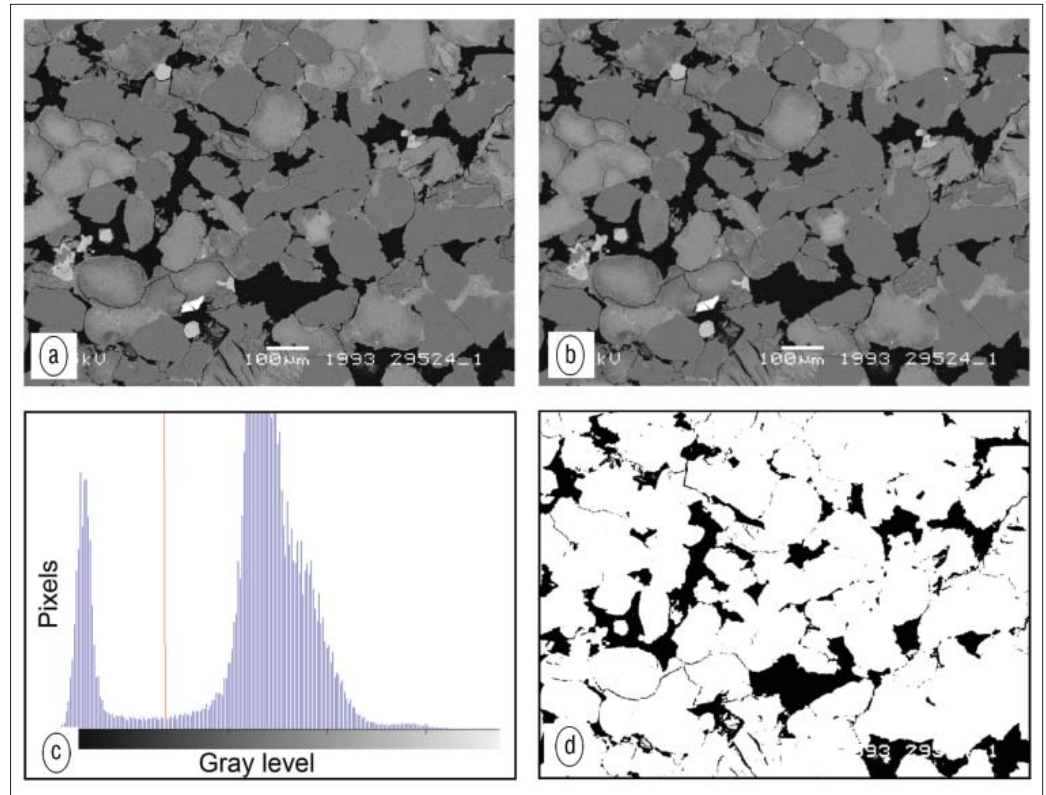
$$E_{dynamic} = 2\rho v_s^2 \left(1 + \frac{(v_p^2 - 2v_s^2)}{2(v_p^2 - v_s^2)} \right) \quad (3)$$

and the dynamic Poisson's ratio becomes:

$$\nu_{dynamic} = \frac{(v_p^2 - 2v_s^2)}{2(v_p^2 - v_s^2)} \quad (4)$$

Permanent deformation of the medium may be quantified by image analysis of backscatter micrographs. Changes in

Figure 3. Measuring macroporosity by image analysis: (a) original image, (b) filtered image when noise level is reduced, (c) histogram of gray level and setting a threshold (red) to create a binary image, and (d) binary image where black pixels represent pores and white pixels represent grains. These procedures were done using MATLAB code.



macroporosity indicate sliding and rearrangement of grains, and changes in grain shape indicate permanent deformation of grains. Grain shape may be quantified as roundness and sphericity. Roundness is calculated from the area (A) and perimeter (P) of a grain:

$$\text{Roundness} = \frac{4\pi A}{P^2} \quad (5)$$

Sphericity is calculated from the semimajor axis (a), and semi-minor axis (b), of a grain:

$$\text{Sphericity} = \frac{2\sqrt[3]{ab^2}}{a + \frac{b^2}{\sqrt{(a^2 - b^2)}} \ln\left(\frac{a + \sqrt{(a^2 - b^2)}}{b}\right)} \quad (6)$$

Testing

Compression to an axial stress of 15 MPa is done in a tri-axial cell (Figure 2), while confining pressure is manually controlled to 2 MPa. The sample is drained during measurements, so the pore pressure is equal to the atmospheric pressure at the low deformation rate of $3 \times 10^{-6} \text{ s}^{-1}$ (1% per hour). Axial and radial strains are measured by strain gauges glued to the sample. Data are sampled with an interval of 5 s. Ultrasonic P-wave and S-wave velocity are measured with a center frequency of 132 kHz. Within the steel pistons of the triaxial cell piezoelectrical crystals are embedded so that acoustic measurements can be done continuously during the compression test.

Grain density is measured by He porosimetry, and the initial and final porosity calculated from sample dimensions of the plug before testing and mercury immersion of the sample

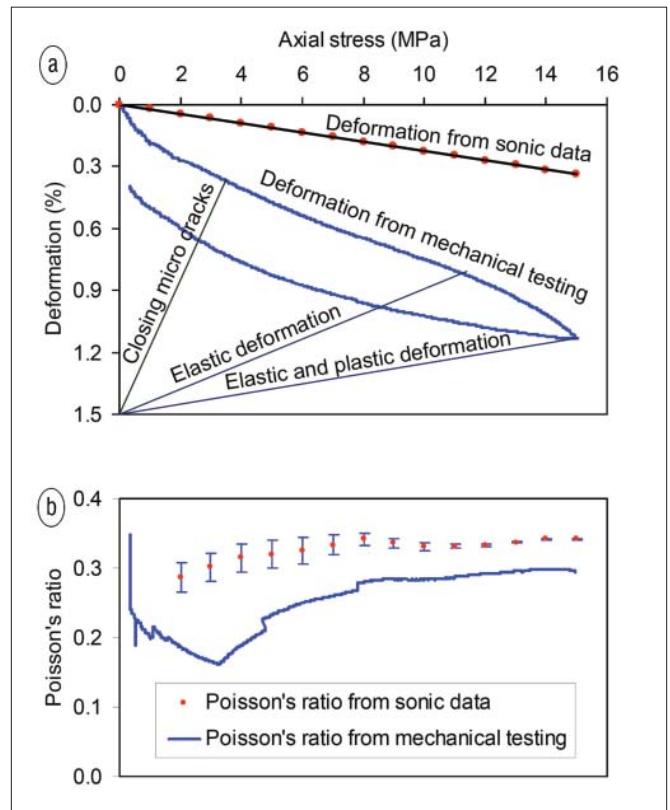


Figure 4. (a) Elastic deformation calculated from sonic data and elastic and nonelastic deformation from uniaxial compression test. Data for uniaxial compression test are obtained after the first cycle in order to minimize influence of microcracks. (b) Static and dynamic Poisson's ratios for greensand sample. Static Poisson's ratio data below 2 MPa are unreliable due to the effect of confining pressure.

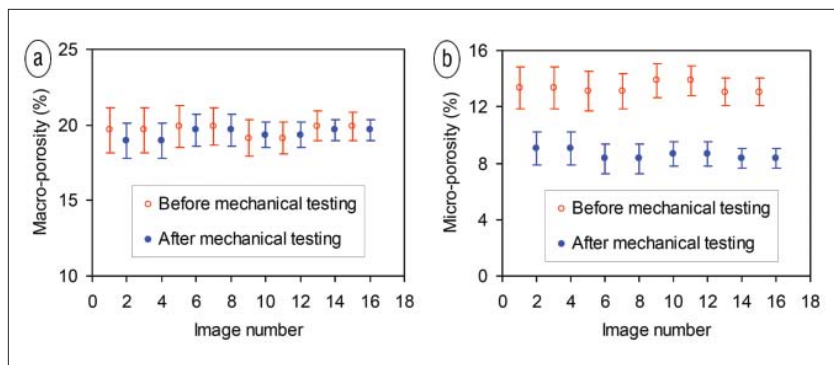


Figure 5. Comparison of changing macroporosity and microporosity as measured by image analysis. (a) Macroporosity is practically unchanged by mechanical testing. (b) Microporosity within glauconite decreases by mechanical testing.

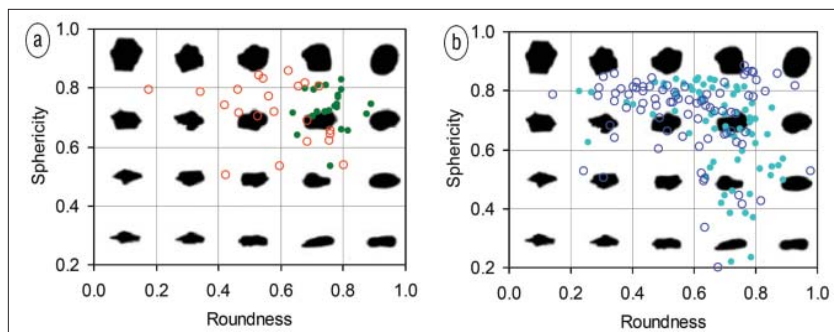


Figure 6. Calculated roundness and sphericity of grains before and after geomechanical testing: (a) glauconite grains and (b) quartz grains. Glauconite grains are more rounded and more flattered after geomechanical testing. For quartz grains no significant change was observed. (Figure background modified after Krumbein and Sloss.)

after testing. Electron micrographs of polished thin sections are used for image analysis to measure macroporosity, grain roundness, and grain sphericity before and after testing (Figure 3).

As is normally the case for porous media, the deformation obtained from geomechanical testing is higher than would be expected from the dynamic $E_{dynamic}$ obtained from sonic data (Figure 4). When the resulting permanent strain ($d\epsilon_{nonelastic}$) is taken into account, we find that the elastic strain corresponds to:

$$d\epsilon_z = d\epsilon_{elastic} + d\epsilon_{nonelastic} \quad (7)$$

and that the elastic strain is higher than the strain predicted from sonic data by a factor 1.3–3. When the elastic strain is measured from the loading curve we find that:

$$d\epsilon_{elastic} = 3d\epsilon_{dynamic} \quad (8)$$

whereas when the elastic strain is measured from the unloading curve we find:

$$d\epsilon_{elastic} = 1.3d\epsilon_{dynamic} \quad (9)$$

This confirms the common observation that Young's modulus is higher in the dynamic case than in the static case. The lower factor from the unloading curve (Equation 9) indicates that

the loading is not purely elastic, but includes some degree of plastic deformation, whereas the unloading curve may be closer to truly elastic. Poisson's ratio also becomes higher in the dynamic case. From the unloading curve we find:

$$1.2 v_{elastic} = v_{dynamic} \quad (10)$$

It should be borne in mind that deformation measured by strain gauges may underestimate the total volumetric deformation. Core analysis data indeed indicate that due to permanent nonelastic deformation, the total porosity of the sample is reduced from 33% to 30%.

From image analysis we find that the permanent deformation is due to deformation of the glauconite grains and consequent reduction in microporosity rather than reduction in macroporosity (Figure 5). We find that due to the geomechanical testing, the shape of the glauconite grains has changed so that the average sphericity has decreased. By contrast quartz grains have maintained their shape (Figure 6).

Conclusions

Combining information from geomechanical testing, sonic velocity and image analysis of backscatter electron micrographs can give information on which grains in a sandstone suffers elastic deformation and which grains suffer plastic deformation.

We applied this method to an oil-zone sample from a North Sea Paleocene greensand with 20% macroporosity and 13% microporosity and found that loading to 15 MPa under uniaxial conditions resulted in 0.45% elastic deformation and from volumetric strain 1% plastic deformation. The plastic deformation is caused by permanent deformation of the glauconite grains only, so that microporosity decreases whereas macropores and quartz grains only deform elastically.

When taking the plastic deformation into account, Young's modulus determined by geomechanical testing is 1.3 to 3 times smaller than Young's modulus calculated from sonic data, and Poisson's ratio correspondingly is 1.2 times smaller when it is determined from geomechanical testing than when it is calculated from sonic data.

Suggested reading. "Paleocene" by Ahmadi et al. (*The Millennium Atlas: Petroleum Geology of the Central and Northern North Sea*, Geological Society Publishing House, 2003). "Static and dynamic Young's moduli of chalk from the North Sea" by Olsen et al. (GEOPHYSICS, 2008). *Stratigraphy and Sedimentation* by Krumbein and Sloss (Freeman, 1963). **TLE**

Corresponding author: zah@env.dtu.dk